ULTRAFAST SUPERCONTINUUM LASER SOURCE

PHOTONICS SPECTRA, 11, 53, 1984

TECHNOLOGY TRENDS

ULTRAFAST SUPERCONTINUUM LASER SOURCE

BY J. T. MANASSAH, P.P. HO, A. KATZ AND R.R. ALFANO

Super-continuum generation, the production of intense, fast broadband pulses by passing a picosecond laser pulse through certain media, was demonstrated 14 years ago by Alfano and Shapiro.[1] The ultrafast supercontinuum laser source (USLS) is generated from self-phase modulation (SPM). Typically it produces an output frequency ranging over 10,000cm^{-1} on either side of the pump laser frequency and a pulse duration on the order of 100 femtoseconds (100×10^{-15}s). The shape, fine structure and extent of the spectrum produced by a USLS are functions of the nonlinear index of refraction of the medium, the shape, wavelength, duration intensity

Now this laser source looks good for ranging, imaging, remote sensing and optical fiber measurements.

and phase modulation of the pump laser pulse, and the interaction length of the pulse in the medium. Recently, Shank and coworkers[2] have confirmed Alfano and Shapiro's work, finding that SPM is responsible for the generation of the supercontinuum in liquids and solids.

The optical properties of the USLS, such as coherence and pulse duration, are determined by the pump laser. Figure 1 shows the spectral emission from a carbon tetrachloride USLS, triggered by a 120fs excitation pulse at 625nm. Over 90 percent of the input energy has been converted into the continuum light. Recently, applying Treacy's[3] pulse compression technique, SPM has been used to compress picosecond pulses into the femtosecond region.[4] A theoretical analysis of SPM is included in the boxed story accompanying this article.

The coherent and ultrafast wide-frequency band of the USLS can be applied in those instances where a knowledge of specified phase and intensity for well-separated wavelengths is advantageous. It simplifies experiments that measure time delay and relative intensity for different wavelengths simultaneously. In the past, the "supercontinuum" has been mainly used as a spectral tool for time-resolved absorption spectroscopy[5,6] and nonlinear optical effects.[5,7] Here, however, we establish new uses for USLS in ranging, imaging, atmospheric remote sensing and optical fiber measurements.

In the regime where the dominant effect of nonlinearity is self-phase modulation, a pulsed laser pump can produce a spectral distribution such that the intensity for each line is well defined and all lines in the spectrum are emitted within a time uncertainty equal to the pulse width (see the figure in the boxed section). Frequency bands located within the pulse duration can be separated in time if the dispersive effects in the material are reduced.

New applications: ranging

The main limitation to the accuracy of optical length measurements through the uncontrolled atmosphere is the uncertainty in the average refractive index over the optical path due to nonuniformity and turbulence of the atmosphere. Simultaneous measurements over the same path using two or more different wavelengths of light could be used to provide the base values. The dispersive delays between any two wavelengths can be calculated using Owens'[8] expressions for the dependence of the optical refractive index of air as a function of the ambient pressure, temperature and composition.

This research is funded in part by AFOSR, ARO, NASA and NSF.

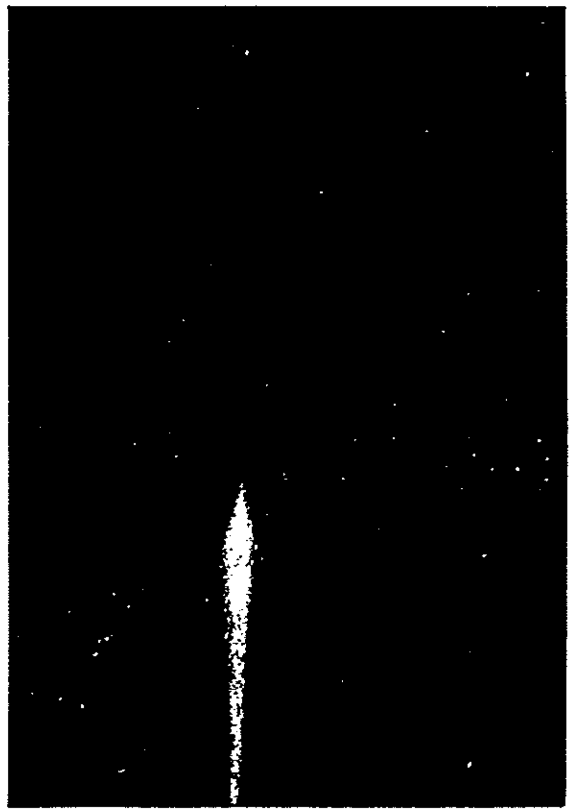

Figure 1.
The relative USLS emission intensity vs. wavelength for one millimeter of carbon tetrachloride excited by a 120fs, 625nm laser pulse.

For path lengths of a few tens of meters, Erickson[9] proposed the use of direct interferometry for dispersive delay measurements. In effect, this type of system consists of an automatic fringe-counting Michelson interferometer. But for lengths larger than one hundred meters, direct interferometry is impractical.

For distances of a few kilometers, a system using a pulsed, subpicosecond, single-wavelength laser source and a synchroscan streak camera with a 3ps time resolution as a detector can be used. If the index of refraction of the ambient air is known to an accuracy of 0.1ppm, this type of system will measure to an accuracy of a millimeter. However, the index of refraction of air varies by as much as 100ppm over the operational range of such rangefinders, and the measurement accuracy is thus reduced to ± 1 meter. (The time delay between two signals in different media is $\Delta\tau = (L/c)\delta n$).)

On the other hand, if a system consists of a multiwavelength source, such as a USLS, and a multichannel synchroscan streak camera[8] in the receiver, the arrival

THEORETICAL ANALYSIS OF SELF-PHASE MODULATION

In this section, we review the theory of the SPM-generated spectrum.* The optical electromagnetic field propagating in a medium satisfies the vector wave equation implied by Maxwell's equations:

$$\nabla \times \nabla \times \vec{E} + \frac{1}{c^2}\frac{\partial^2 \vec{E}}{\partial t^2} = -\frac{4\pi}{c^2}\frac{\partial^2 \vec{P}}{\partial t^2} \quad (1)$$

The polarization density is given by a linear and nonlinear part:

$$\vec{P} = \vec{P}^{L} + \vec{P}^{NL} \quad (2)$$

The linear part of the polarization is related to the usual susceptibility through:

$$\vec{P}^{L}(\vec{x},\omega) = \chi(\omega)\,\vec{E}(\vec{x},\omega) \quad (3)$$

We are interested in the propagation of nearly monochromatic pulses of light, for which the amplitude E is given by:

$$\vec{E} = \mathrm{Re}\ \vec{E}(\vec{x},t)\, e^{-i\omega_0 t} e^{ik_0 z}. \quad (4)$$

and E varies little in a period $2\pi/\omega_0$.

Omitting derivatives of E with respect to t of third order and higher, and those with respect to z of second order and higher, and using the expression for the index of refraction at ω_0:

$$c^2 k_0^2 = [1 + 4\pi\chi(\omega_0)]\,\omega_0^2 = n^2\omega_0^2 \quad (5)$$

the wave equation for the field amplitude is

$$\nabla_T^2 E + 2ik_0\left(\frac{\partial}{\partial z} + \frac{1}{v_g}\frac{\partial}{\partial t}\right)E - \frac{G}{v_g^2}\frac{\partial^2 E}{\partial t^2}$$

$$= -\frac{4\pi}{c^2}\left(\omega_0 + i\frac{\partial}{\partial t}\right)^2 P^{NL} \quad (6)$$

where the group velocity v_g is:

$$(v_g)^{-1} = \frac{d}{d\omega}\left(\frac{n\omega}{c}\right), \quad (6a)$$

and

$$G = 1 - k_0\frac{\partial v_g}{\partial \omega}. \quad (6b)$$

The simplest form of the general third-order nonlinear polarization for isotropic media is:

$$P^{NL} = \eta |E|^2 E \quad (7)$$

In equation 6, the $\nabla_T^2 E$ term is responsible for self-focusing, the $\partial^2 E/\partial t^2$ term is responsible for dispersive pulse distortion, and in cases of anomalous dispersion:

$$\left(\frac{1}{v_g^2}\frac{\partial v_g}{\partial \omega} > 0\right)$$

this term is responsible for self compression, and the time derivatives of P^{NL} are the corrections to the inertialess model

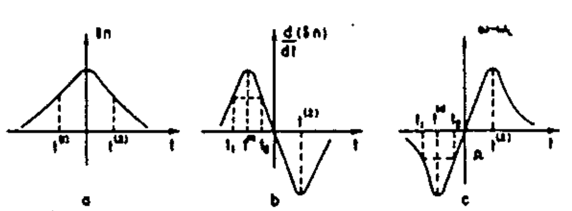

SPM mechanism: a. Nonlinear index change vs. time; b. time rate of change of index change; c. frequency change vs. time. $t^{(1)}$ and $t^{(2)}$ are the inflection points of δn. t_1 and t_2 are the critical points (i.e., the roots of equation 12).

for nonlinearity. In instances where these terms are assumed small, eq. 6 reduces to the standard self phase modulation equation given by:

$$ik_0\left(\frac{\partial}{\partial z} + \frac{1}{v_g}\frac{\partial}{\partial t}\right)E = -\frac{2\pi\omega_0}{c^2}\eta|E|^2 E. \quad (8)$$

Introducing the new variable $t' = t - z/v_g$, the solution of the above equation is given by:

$$E(z,t') = E_0(t')\exp\left[i\left[n_2\omega_0\left|E_0(t')\right|^2\frac{z}{2c}\right]\right]. \quad (9)$$

where the nonlinear index of refraction is

$$\delta n \approx \frac{1}{2}n_2\left|E\right|^2 \text{ and } n_2 = \frac{4\pi}{n}\eta.$$

The detected intensity in the frequency domain range from ω to $\omega + \Delta\omega$ is:

$$I_\omega \Delta\omega = \frac{nc}{4\pi^2}\frac{1}{T_S}\int_\omega^{\omega+\Delta\omega}\left|\tilde{E}(\omega-\omega_0)\right|^2 d\omega,$$

where T_S is the time available to determine the spectrum. If T_S is very long:

$$\tilde{E}(z,\omega-\omega_0) = \int_{-\infty}^{\infty} dt E(z,t)\, e^{i(\omega-\omega_0)t}. \quad (10)$$

If the phase of E (z,t) becomes large compared with π, the method of stationary phase can then be utilized to evaluate the Fourier component. Denoting the phase of E (z,t) by ϕ, then:

$$\tilde{E}(z,\omega-\omega_0) \approx \Sigma_\nu E_0(t_\nu)e^{i\phi_\nu}e^{i(\omega-\omega_0)t_\nu}e^{i\pi/4}\left[\frac{2\pi}{\phi_\nu''}\right]^{1/2} \quad (11)$$

where t_ν is the νth root of

$$\omega(t) = \omega_0 - \frac{\partial\phi}{\partial t}\, t \quad (12)$$

and ϕ_ν and ϕ_ν'' are the phase function and its second derivative at t_ν. For an incoming Gaussian pulse given by:

$$E_0(t) = E_0\exp\left[-t^2/T_p^2\right] \quad (13)$$

the modulation frequency of the SPM spectrum is:

$$\delta\omega = \frac{2.4\pi}{T_p} \quad (14)$$

and the maximum frequency extent is

$$\left|\Delta\omega_{max}\right| \sim \frac{\omega_0 n_2}{(2\ell n 2)^{1/2}\, c\, T_p} E_0^2 z \quad (15)$$

which indicates that the frequency extent is inversely proportional to T_p (i.e., the shorter the incoming pulse, the greater is the frequency extent), and linear in n_2, E_0^2 and z. For femtosecond pulses, $\Delta\omega$ extends over 10,000 cm^{-1} in the UV, visible and IR regions. The figure shows the temporal development of continuum generations — red leads blue.

*Alfano, R.R., L. Hope and S.L. Shapiro (1972). *PHYS. REV. LETT.* A6:43; also Ostrovskii, L.A. (1967). *JETP LETT.* 6:260; also Shimuzu, F. (1967). *PHYS. REV. LETT.* 19:1097; also, Cubeddu, R., et al. (1970). *PHYS. REV.* A2:1955; also Marburger, J.H. (1975). *PROG. QUANT. ELECTR.* 4:35.

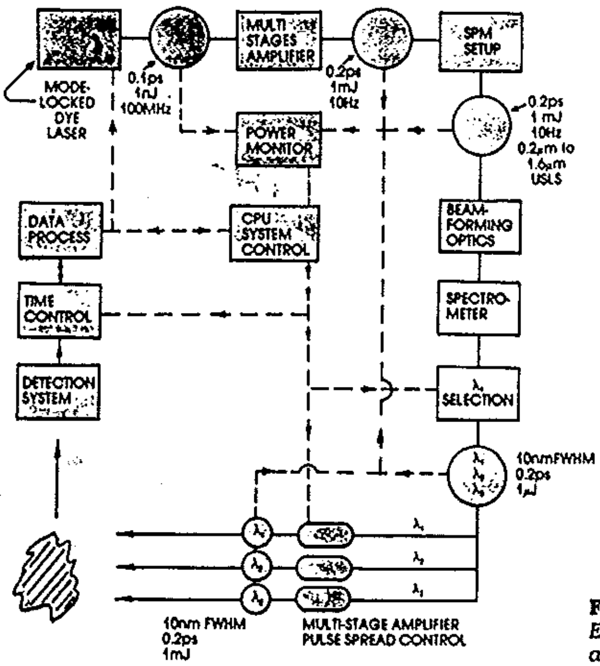

Figure 2.
Experimental setup of USLS for remote sensing applications.

time data for the different wavelengths determines the parameters in the Owens index of refraction formula (wavelength, temperature, pressure and relative humidity dependence) to an accuracy of 0.4ppm. Consequently, the accuracy of the distance measurements is restored to the $\pm$0.4cm range. Simultaneously, the pressure can be determined to an accuracy of 1.5mbar and the temperature to $\pm$0.5°K. Furthermore, the wide frequency band of the USLS allows for the selective tuning and encoding (for example, the addition of a constant phase) of the different emitted lines. This provides the added feature of system integrity under adverse field conditions, such as jamming or interference.

3D imaging

The direct, nondestructive, *in situ* measurement of an object's surface contour as well as its internal structure can be accomplished with an accuracy of 30µm using 100-femtosecond laser pulses to produce a continuum. In such a system, reflections from surface imperfections are delayed with respect to reflections from other surface points, and thus will be sensed by a detector at different times. Experimentally, measurements are carried out by modulating arrival times to the target using an oscillating delay prism and passing the reflected signal together with a reference signal into a second-harmonic correlation crystal. The convoluted harmonic signal is then detected by a video system in synchronism with the modulation frequency. When three different optical frequencies from the USLS are used and the corresponding beams are collimated in a three-dimensional orthogonal configuration, a three-dimensional image of the imperfection can be directly deduced.

The signal-to-noise ratio for each frequency channel (and the interchannels) is excellent. This technique can measure, for example, semiconductor surfaces, tissue topography and defects and wear on ball bearings.

For diagnostic analysis of an object inside a material, the different reflection and absorption coefficients for the different optical frequencies at the interfaces and in the materials can be used to measure the location and contour of cracks or impurities inside a sample. The accuracy of the measurement can be further enhanced beyond $\pm$30µm by selecting one of the frequencies to be close to a resonance line, thus endowing it with a large optical path in the medium, which in turn results in longer time delays and more accurate spatial measurements. These techniques can, for example, measure impurity locations inside Si and GaAs. Measurements in polymers and biological and medical samples are also possible.

Atmospheric remote sensing

The use of differential absorption lidar (DIAL) for remote sensing of atmospheric species has been shown to be a viable experimental technique for the detection and identification of a wide range of molecular constituents.[11] The lidar equation is given by:

$$\frac{P_r}{P_t} = \frac{K\varrho A}{\pi R^2} \exp[-2(\sigma_a(\lambda)N_a + \alpha(\lambda))R]$$

where P_r and P_t are respectively the received and transmitted powers, K is the overall system efficiency, ϱ is the target reflectivity, A is the receiving telescope area, σ_a is the absorption cross section of the absorbing molecule a, R is the range and α is the background extinction coefficient of the atmosphere. A measurement of N_a based on a single wavelength requires an accurate knowledge of K, ϱ, α and σ_a. However, K, ϱ and α are generally known with only a poor accuracy.

The differential absorption lidar[10] approach attempts to overcome some of these difficulties by performing the lidar experiment with two or more frequencies. For a dual-wavelength source with frequencies $\nu^{(1)}$ and $\nu^{(2)}$,

$$N_a = \frac{1}{2(\sigma_a^{(2)} - \sigma_a^{(1)})R}\left[\ln\left(\frac{P_a^{(1)}}{P_a^{(2)}}\right) - \ln\left(\frac{\varrho^{(2)}}{\varrho^{(1)}}\right) - 2(\alpha^{(1)} - \alpha^{(2)})R\right]$$

where $P_a = P_r/P_t$ and the superscript refers to the wavelength. A multi-wavelength source (such as the continuum SPM-generated USLS) with built-in calibrated power spectrum provides the possibility of a more ac-